JCTC Journal of Chemical Theory and Computation

Implementation of the CHARMM Force Field in GROMACS: Analysis of Protein Stability Effects from Correction Maps, Virtual Interaction Sites, and Water Models

Pär Bjelkmar,[†] Per Larsson,[†] Michel A. Cuendet,[‡] Berk Hess,[†] and Erik Lindahl*,[†]

Center for Biomembrane Research, Department of Biochemistry & Biophysics, Stockholm University, SE-106 91 Stockholm, Sweden, and Molecular Modeling Group, Swiss Institute of Bioinformatics, CH-1015 Lausanne, Switzerland

Received October 16, 2009

Abstract: CHARMM27 is a widespread and popular force field for biomolecular simulation, and several recent algorithms such as implicit solvent models have been developed specifically for it. We have here implemented the CHARMM force field and all necessary extended functional forms in the GROMACS molecular simulation package, to make CHARMM-specific features available and to test them in combination with techniques for extended time steps, to make all major force fields available for comparison studies in GROMACS, and to test various solvent model optimizations, in particular the effect of Lennard-Jones interactions on hydrogens. The implementation has full support both for CHARMM-specific features such as multiple potentials over the same dihedral angle and the grid-based energy correction map on the ϕ, ψ protein backbone dihedrals, as well as all GROMACS features such as virtual hydrogen interaction sites that enable 5 fs time steps. The medium-to-long time effects of both the correction maps and virtual sites have been tested by performing a series of 100 ns simulations using different models for water representation, including comparisons between CHARMM and traditional TIP3P. Including the correction maps improves sampling of near native-state conformations in our systems, and to some extent it is even able to refine distorted protein conformations. Finally, we show that this accuracy is largely maintained with a new implicit solvent implementation that works with virtual interaction sites, which enables performance in excess of 250 ns/day for a 900-atom protein on a quad-core desktop computer.

Introduction

Utilizing a force field that is as accurate as possible is one of the most important factors when using molecular dynamics to predict different macromolecular properties. The past decade has seen significant advances in force field development, and with this, many of them have become increasingly precise and accurate for predictions of nontrivial properties such as structure, dynamics, or free energies. One of the most prominent improvements in contemporary force fields has come from adjusting parameters to match quantities obtained from quantum mechanical calculations. This has, for instance, been done for the AMBER-99,[1] AMBER-03,[2] GROMOS,[3] and CHARMM22[4] force fields. The major difference between the AMBER-99 and AMBER-03 force fields, for example, includes a reparameterization of charges and dihedral angle parameters, using accurate quantum chemistry potentials together with an implicit solvent model. The idea behind this was to better mimic the internal environment of a protein, where the dielectric constant differs from either an aqueous environment or one in vacuo. Even before this, the Jorgensen group (and later Friesner) developed the OPLS-AA force field,[5,6] where a key idea was to fit parameters to

* Corresponding author e-mail: lindahl@cbr.su.se.
[†] Stockholm University.
[‡] Swiss Institute of Bioinformatics.

10.1021/ct900549r
Published on Web 01/25/2010

better reproduce the entire Ramachandran diagram for amino acids, rather than just individual dihedral potentials.

Some years ago, MacKerell et al.[7] used an analogous but more elaborate idea. The authors looked at how good CHARMM22 was at reproducing quantum chemical potential landscapes for small dipeptide fragments and characterized the deviations between the force-field-based and quantum chemistry energy landscapes. This led to the development of a grid-based energy correction map for protein backbone ϕ and ψ dihedral angles, named CMAP, that enables almost arbitrarily smooth corrections to the Ramachandran map energy landscape. In particular, it no longer has to be a linear superposition of the constituent dihedral potentials. This correction term was implemented in the most recent version of their force field, CHARMM27.[7]

The aim of this work has been to implement these types of potentials in GROMACS, to provide an efficient (GROMACS) reference implementation of the CHARMM27 force field using them, and to assess the accuracy of force field and correction map terms when combined with the water models available in GROMACS. The present implementation supports all major CHARMM27 features, including Urey−Bradley potentials, multiple potentials over the same dihedral angle, and arbitrary correction maps for pairs of dihedrals. This support is obviously highly useful merely as another high-quality choice for large-scale parallel simulations that enables access to a wider set of parameters, and the inclusion of support for all major force fields in the GROMACS distribution will facilitate future systematic comparisons between different force fields for lipids and proteins and help determine how good these are at predicting experimental properties, to what extent they can improve protein structure, and not least how different techniques for higher performance affect various force fields.

It is also an important question to what extent these results are affected by the choice of water models. CHARMM frequently uses an extension of TIP3P with Lennard-Jones interactions also on the hydrogen atoms; while the difference from the classical TIP3P model is minimal, it can be quite significant from a performance point of view since GROMACS can use custom accelerated kernels for traditional water models. To address this, we have compared how the models affect both properties of pure water as well as protein stability assessed through rmsd (coordinate root-mean-square displacement) and dihedral angles. The rmsd is not an entirely unproblematic measure since one is comparing to a packed crystal structure with less water at a much lower temperature, but for better or worse it is still one of the most widely used quality indicators, and it is interesting to see how much force fields in general have improved compared to a decade ago.[8]

Finally, we combine CMAP and the CHARMM27 force field with a new implementation of virtual interactions better suited for all-atom force fields. The use of virtual interaction sites is a technique that goes beyond bond constraints and removes all independent hydrogen atom *degrees of freedom*—but not their interactions—by replacing hydrogens with interaction sites calculated from the heavy atoms to which they are connected.[9] Together with constraints on all bond lengths, this enables time steps of 4−5 fs without an apparent loss of accuracy even for water simulations, and possibly even larger for implicit solvent models.

The stability and accuracy of such "fast" calculation models is particularly critical in the context of protein structure refinement (improving models generated by homology modeling for example). Full protein folding requires exhaustive phase space sampling and is still obviously impossible for all but the very smallest proteins, and even then it requires months of simulation time, which makes it impossible to use in a high-throughput environment. However, it has been shown that, in some cases, with the use of efficient sampling techniques and lots of computer power, molecular dynamics simulations can help refine initially reasonable protein models toward their native state,[10] as measured by rmsd. It is worth noting that practical refinement capability is not necessarily the same as strict model accuracy. Ultimately, one would like the phase space sampling of a simulation starting from a decoy and the native structure to fully converge, but this is still not realistic with a couple of days of simulation time. In practice, the question is rather whether a force field provides an efficient funnel for refinement of structures already in the vicinity of their target. This is likely the main reason for the success of knowledge-based potentials or simple implicit solvent energy minimization techniques in structure refinement, where standard molecular dynamics simulations sometimes even deteriorate the structure.[11] Apart from the increased efficiency (and possibly lower noise) of the implicit solvent, one possible reason for this is that accurate and adequate sampling of backbone dihedral angles is key to accurately refining protein structures,[12,13] and thus applying a simple correction term only to those parameters (i.e., CMAP), while leaving the rest of the force field unaffected, is a promising option that seems to work remarkably well in our trials, even in combination with fast implicit solvent models.

Methods

The CHARMM27 force field for proteins and lipids was ported to the force field format used by GROMACS. For most interactions, such as bonds, angles, and Lennard-Jones and Coulomb interactions, this was merely a matter of bookkeeping and converting units. The two programs for instance occasionally differ by a factor of 2 in potential energy definitions.

Some properties of the CHARMM force field are however specific to the CHARMM molecular simulation package.[14] Such features include the ability in the force field to define multiple dihedral potential terms over the same four atoms, some with a multiplicity ≥ 6 (and hence not representable by the Ryckaert−Bellemans function typically used in GROMACS for efficiency reasons). A new dihedral potential energy function was added in GROMACS to allow such a feature; while this does lead to a few repeated floating-point calculations when the same dihedral is calculated twice, it is quite negligible from a performance point of view. CHARMM27 also uses Urey−Bradley terms for many angles; GROMACS has had support for these internally a long time, but we now also generate them automatically with

Table 1. Average Absolute Errors in Potential Energy (kJ/mol)

GROMACS	CHARMM	$\langle \Delta E \rangle$	NAMD	$\langle \Delta E \rangle$
Bond	BONDs	0.00001	BOND	0.00001
Urey−Bradley	ANGLes+UREY-b	0.0001	ANGLE	0.00002
Proper+Improper Dih.	DIHEdrals+IMPRopers	0.00003	DIHED+IMPRP	0.00001
CMAP Dih.	CMAPs	0.00000	CROSS	0.003
LJ-14+LJ (SR)	VDWaals	0.008	VDW	0.003
Coulomb-14+Coulomb (SR)	ELEC	0.002	ELECT	0.0007

the pdb2gmx proprocessing tool when CHARMM27 is selected, and we similarly generate the appropriate (user-selectable) CHARMM termini for polypeptides. In addition, the CMAP correction term was implemented as described by MacKerell et al.[7] The full implementation was tested by performing single-point potential energy calculations on small (four residues long) homopeptides, and energies were compared to those obtained in the native CHARMM software. This was done for all of the 20 essential amino acid residues. Then, the potential energy was split into corresponding parts (bonds, angles, electrostatics, etc.) and the absolute average error calculated in each case (Table 1).

In the original CMAP implementation, results were assessed using three proteins with PDB identifiers 1GRP, 1HIJ, and 1UBQ. To further validate and test our force field port, we were looking for a different protein with similar properties, that is, being relatively short, having a high-resolution structure, and containing both α-helix and β-sheet regions but no disulfide bridges (since those would stabilize the structure). One of the proteins that fulfilled these criteria was an IgG-binding domain from a streptococcal protein G with PDB identification 1IGD.[15] To probe the effect of the CMAP term on long timescales, as well as different water models and time steps, we used a total of 16 simulation systems, including four simulations to test refinement. The remaining 12 differ in the choice of water model (original TIP3P, CHARMM-modified TIP3P, TIP4P, implicit solvent) and the length of the time step (2 or 4 fs when using explicit solvent, 5 fs with implicit solvent). All simulations extended to 100 ns each, giving an aggregated simulation time of 1.6 μs.

Peptide Setup. Homopeptides with a length of four residues were generated using PyMOL.[16] In selected cases, a short steepest descent energy minimization was performed to relieve local structural strain. Potential energies were then calculated in vacuo without cutoffs to avoid any bias from different definitions of neighbor searching and interaction cutoffs between the two packages.

System Setup. The PDB structure 1IGD was downloaded from the Protein Data Bank,[17] and the first three, unordered, residues were deleted because their lack of a well-defined structure could potentially complicate the evaluation of the CMAP effect. The solvent water was modeled in four different ways: TIP3P and TIP4P,[18] the special CHARMM TIP3P model[4] (with LJ interaction sites also on the hydrogens), and the OBC[19] implicit solvent model, recently implemented in GROMACS. Neutral NH_2 and COOH termini were used, and crystal waters were retained in the systems with explicit water. The protein was placed in a rhombic dodecahedral unit cell with a minimum distance of 1.0 nm to the box edge. Steepest descent minimization was performed followed by an addition of ions to physiologically relevant levels and in order to counterbalance the protein charge, yielding a final system of about 8800 water molecules and 19 Na^+ and 17 Cl^- ions. Finally, another steepest descent minimization was performed. Electrostatics was treated with particle-mesh Ewald (PME),[20] using a short-range cutoff of 1.2 nm, and van der Waals interactions were switched off between 1.0 to 1.2 nm. Temperatures were maintained using the thermostat of Bussi et al.[21] Periodic boundary conditions were applied, as well as isotropic pressure-coupling to a Parrinello−Rahman barostat[22] with a coupling constant of 1 ps. Simulations were run using a 2 fs (TIP3P, CHARMM TIP3P, TIP4P), 4 fs (TIP3P), or 5 fs (OBC) time step, with neighbor list updates every 20 fs.

System Equilibration. The systems were taken through two sets of equilibration simulations, using molecular dynamics (MD) or stochastic dynamics (SD) integration in systems with explicit and implicit solvent, respectively. First, a 2 ps simulation at 240 K was performed followed by a 1 ns simulation at the target temperature of 300 K. The constant for temperature coupling was 1.0 ps in the MD simulations, while the inverse friction constant of the SD integration was set to 91 ps^{-1}, in accordance with previous studies.[23] All covalent bonds were constrained to their equilibrium values by using the P-LINCS[24] algorithm, enabling a 2 fs time step in those cases, whereas in simulations with virtual sites, the time step could be pushed to 4 or 5 fs with the explicit and implicit water models, respectively.[9] For the explicit solvent simulations, all interactions were calculated as for the water system described above, while the implicit solvent simulations were run without cutoffs. Distorted structures for refinement were generated by running simulations at an elevated temperature (1500 K), starting from the energy-minimized protein. Two distorted structures were used, one with a 0.2 nm root-mean-square deviation (rmsd) of backbone heavy atoms and one with 0.3 nm. To study water structural effects, systems with 1000 previously equilibrated water molecules were simulated for 100 ns using all four different water models.

Improved Virtual Site Construction. Virtual interaction sites (originally called "dummies") have been available in GROMACS for almost a decade.[9] Their definition is quite straightforward: The virtual site coordinates are calculated from a set of constructing atoms every step. It takes part in the normal force evaluation, and finally the forces are spread back onto the constructing atoms by simply using the construction equations for the coordinates together with the derivative chain rule. In terms of energy conservation, the virtual site construction itself is perfect (the force is

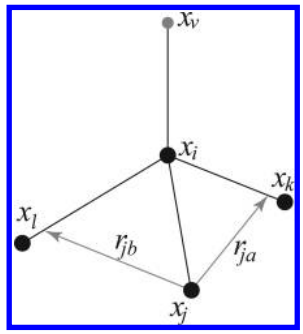

Figure 1. New tetrahedral virtual site type from four atoms that is stable even when the constructing atoms *i*, *j*, *k*, and *l* are close to planar. See eq 1 for a formal definition.

exactly the derivative of the potential with respect to the constructing coordinates), but the potential for accuracy/speedup is limited by (1) whether the removed degrees of freedom were important and (2) the next fastest motion that limits the time step. Unfortunately, while the original virtual site approach was remarkably stable for force fields that only included polar hydrogens, it could occasionally cause errors with all-atom force fields. This was traced down to a particular construct (4FD of Feenstra et al.) used to build nonpolar protein H_α atoms from C_α, C_β, N, and O; in the extremely rare case of the four constructing atoms being almost in a plane, this construct (but no others) can become unstable. We have corrected this by implementing a new 4FDN type. Assuming the virtual site $\mathbf{x}_v$ is connected to the tetrahedral center $\mathbf{x}_i$, which in turn is connected to $\mathbf{x}_j$, $\mathbf{x}_k$, and $\mathbf{x}_l$, the new virtual site is defined from three scalar parameters a, b, and c as (see Figure 1)

$$\begin{aligned} \mathbf{r}_{ja} &= a\mathbf{r}_{ik} - \mathbf{r}_{ij} = a(\mathbf{x}_k - \mathbf{x}_i) - (\mathbf{x}_j - \mathbf{x}_i) \\ \mathbf{r}_{jb} &= b\mathbf{r}_{il} - \mathbf{r}_{ij} = b(\mathbf{x}_l - \mathbf{x}_i) - (\mathbf{x}_j - \mathbf{x}_i) \\ \mathbf{r}_m &= \mathbf{r}_{ja} \times \mathbf{r}_{jb} \\ \mathbf{x}_v &= \mathbf{x}_i + c\frac{\mathbf{r}_m}{|\mathbf{r}_m|} \end{aligned} \quad (1)$$

While this is somewhat more expensive to calculate (in particular, the analytical derivatives) due to the usage of the cross product, it is negligible for practical simulations, and this construct type has no stability issues.

Results

For testing the correctness of the force field implementation, we compared the values for the potential energy of all amino acids to the force field included in the c33b1 release of CHARMM[14] and NAMD version 2.7b2[25] (Table 1). The CMAP implementation was also validated by comparing forces. These calculations were performed in vacuo without cutoffs, since implementation detail differences between CHARMM and GROMACS make it difficult to get exactly identical results with other setup schemes. For example, CHARMM does not necessarily work with charge groups, switch/shift functions are not the same,[26] and definitions of interaction cutoffs differ as well as rules for neighbor searching.

In analogy with MacKerell,[4] simulations with and without the CMAP correction terms were run to probe its effect. To extend their results and study the effects also on long timescales, simulations of 100 ns were performed. First, average differences between the ϕ and ψ backbone dihedral angles in simulation were calculated relative to the crystal structure, averaged over all residues, as well as split into helical and sheet regions (Table 2). Both signed (as in the reference CMAP article) and unsigned differences were calculated, since the latter will expose systematic differences for individual residues that were canceled by the average over residues. Standard errors were estimated from autocorrelations as described by Hess;[27] while fluctuations can be large in loops and terminini, they are very small in ordered secondary structure regions, with standard errors below 2° in general. The results are consistent with MacKerell et al.; that is, these backbone dihedrals sample regions in conformational space significantly closer to those in the crystal structure when the CMAP term is applied. This is particularly obvious in the ordered secondary structure regions of helices and sheets, where these angles fluctuate around an average close to the crystal structure. Interestingly, this result is generally true for all water models and time steps investigated here. In particular, we could not detect any significant difference between the CMAP simulations that used the original TIP3P model and those with the CHARMM version of TIP3P. Even the implicit solvent simulations benefit from CMAP; the ϕ and ψ angles are only slightly worse than with explicit water, and considerably better than the non-CMAP explicit solvent simulations.

To illustrate the behavior of these dihedral angles over time, Figure 2 shows the average ϕ and ψ absolute differences for all residues for the frames of the 100 ns of production runs of the simulations using the TIP3P water model. Clearly, there are significant changes in the distributions of these angles on a timescale of tens of nanoseconds, which is important when considering lengthscales of refinement simulations, for example. Note that these 100 ns were preceded by 1 ns of nonrestrained equilibration simulations, during which the dihedral angles increased to the levels seen in the beginning of these graphs. As a reference, we also performed simulations with and without CMAP in a vacuum (data not shown) using 2 fs time steps, and as expected, the values of the dihedral differences and the rmsd are significantly worse in both cases. Hence, adding the CMAP term is a subtle effect, not simply overstabilizing the native state since a proper water model is needed for relevant sampling of the protein structure.

The average of the instantaneous rmsd between the crystal structure and the simulations was found to drop when the correction term was applied (Table 3). Again, the simulations using the original and CHARMM versions of the TIP3P water model were in practice indistinguishable, as well as the backbone rmsd of the two simulations with a 4 fs time step and virtual sites (with the original TIP3P). For side chains, which are generally more flexible than backbone atoms, the rmsd (of side chain heavy atoms) decreases when utilizing the virtual sites construction both with and without CMAP. One reason for this could be that the rigid interaction sites serve to make side chains slightly more stiff. Interestingly, there is no significant difference between the simula-

Table 2. Average ϕ, ψ Differences (deg) from Crystal Structure

	CHARMM27				CHARMM27 + CMAP			
system (1IGD)	$\langle\Delta\phi\rangle$	$\langle\lvert\Delta\phi\rvert\rangle$	$\langle\Delta\psi\rangle$	$\langle\lvert\Delta\psi\rvert\rangle$	$\langle\Delta\phi\rangle$	$\langle\lvert\Delta\phi\rvert\rangle$	$\langle\Delta\psi\rangle$	$\langle\lvert\Delta\psi\rvert\rangle$
				All Residues				
TIP3P	0.5	16.5	−10.8	19.8	−1.2	9.3	−4.6	9.8
CHARMM TIP3P	2.8	14.1	−12.0	17.3	−1.4	9.1	−5.6	8.9
TIP4P	2.7	13.5	−12.3	18.6	−0.5	9.5	−6.8	10.3
TIP3P vsites	2.7	13.4	−16.3	22.4	−2.2	8.9	−3.4	8.5
OBC	3.6	14.4	−17.2	21.0	−0.9	12.7	−6.4	15.7
OBC vsites	2.7	14.0	−20.8	24.9	−1.7	11.6	−7.0	15.3
				Helical Residues				
TIP3P	4.1	8.0	−3.7	7.0	0.3	3.4	−0.1	3.5
CHARMM TIP3P	4.2	7.9	−3.8	6.9	0.1	3.1	−0.2	3.6
TIP4P	3.9	8.4	−3.7	7.3	0.3	3.7	0.1	3.5
TIP3P vsites	4.6	8.2	−4.5	7.8	0.2	2.7	−0.4	3.4
OBC	6.3	8.6	−7.4	9.0	2.7	5.6	−1.9	4.1
OBC vsites	7.1	8.9	−7.5	8.8	3.4	5.8	−2.0	3.9
				Sheet Residues				
TIP3P	6.6	11.5	−12.5	17.6	−1.4	8.6	−4.3	7.0
CHARMM TIP3P	5.3	10.5	−10.2	16.8	−1.6	8.8	−4.1	6.9
TIP4P	4.9	8.7	−10.5	17.4	−1.4	9.4	−4.5	7.9
TIP3P vsites	5.3	9.9	−14.5	20.1	−0.8	6.9	−2.5	6.4
OBC	5.7	11.0	−16.5	21.5	−1.4	6.9	−1.9	8.8
OBC vsites	5.0	10.5	−18.2	23.1	−0.7	6.4	−2.6	9.5

tions with the implicit OBC model combined with CMAP compared to the explicit water models, not even when running with virtual sites and 5 fs time steps. Since this setup provides the highest computational performance by far, it is an interesting option for refinement. Also, with implicit solvent and virtual sites, side chains retain the same flexibility as when using only a 2 fs time step and could arguably sample the local conformational space better.

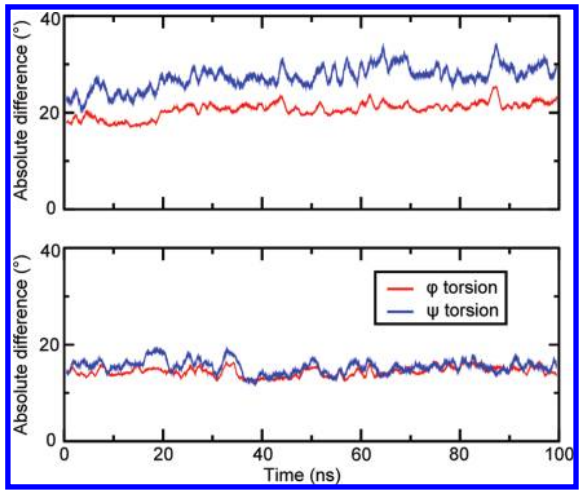

Figure 2. Average absolute differences in the ϕ and ψ backbone torsion angles compared to the corresponding angles in the protein crystal structure for the 100 ns of production runs. To decrease fluctuations, running averages have been computed from 1 ns windows. In this example, simulations were run with the TIP3P water model with and without CMAP, in the lower and upper panels, respectively. The differences in ϕ and ψ are considerably less when applying CMAP.

Table 3. Protein Stability and rmsd (nm) from Crystal Structure

	CHARMM27		CHARMM27 + CMAP	
system (1IGD)	backbone	side-chain	backbone	side-chain
TIP3P	0.12	0.23	0.09	0.20
CHARMM TIP3P	0.11	0.22	0.09	0.20
TIP4P	0.11	0.23	0.09	0.21
TIP3P vsites	0.12	0.18	0.09	0.15
OBC	0.11	0.23	0.09	0.20
OBC vsites	0.13	0.23	0.09	0.21

Table 4. Protein G rmsd (nm) after Refinement

	CHARMM27 + CMAP	
system (1IGD)	from 0.2 nm	from 0.3 nm
TIP3P	0.11	0.28
OBC vsites	0.09	0.20

To investigate this further, we performed an elevated-temperature run in explicit water (again using the same protein, see the Methods section) to obtain structures to refine. Starting from a conformation that is initially 0.3 nm away from the crystal structure, we reach a rmsd of 0.28 nm with explicit water (calculated over the last 10 ns of a 100 ns simulation). The implicit solvent simulation does considerably better at approximately 0.20 nm. For the structure that started at 0.2 nm, we reach final values of 0.11 nm (explicit water) and 0.09 nm (implicit water; Table 4, Figure 3). While this at first sight appears to be identical to the value starting from the crystal structure, it has (unsurprisingly) not converged to cover the same phase space. When instead comparing the rmsd of *average structures*, the whole TIP3P explicit-water simulation reaches a remarkably low 0.055 nm; the last 10 ns of the explicit-water refinement starting from 0.2 nm reaches 0.09 nm, but the difference between the two is still 0.08 nm. Despite nonfully converged phase spaces, we believe this is promising for future refinement work.

Implicit solvation makes the sampling of conformational space faster as all solvent degrees of freedom are averaged out, indicating that it can move a structure far away (0.3 nm) from the conformation in the crystal structure faster

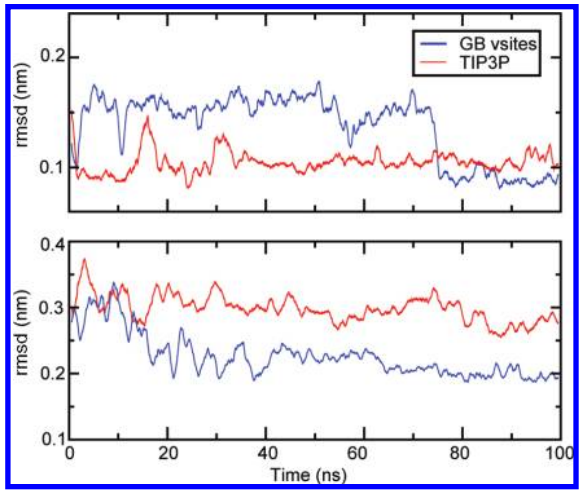

Figure 3. The rmsd of refinement simulations for the 1IGD system with explicit TIP3P water molecules in red and the implicit OBC model and hydrogen virtual sites in blue. Curves were smoothened by running averages from windows of 1 ns length. The rmsd is followed for simulations starting from a protein conformation 0.2 and 0.3 nm from the crystal structure, shown in the upper and lower panels, respectively.

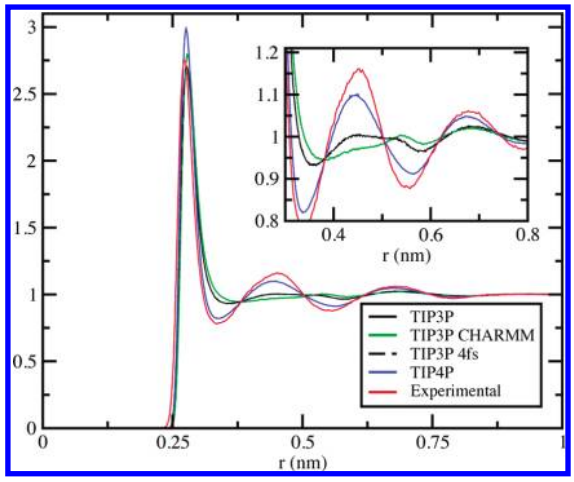

Figure 4. Radial distribution functions for oxygen−oxygen distances for the different water models. TIP4P is closest to the experimental reference curve.[28] Using TIP3P with a 4 fs time step yields a RDF (dashed) that is indistinguishable from that with a 2 fs time step.

toward this state. Starting closer to the native state (0.2 nm), the protein structure is again clearly closer to the crystal conformation at the end of the simulations, but there is less difference between explicit and implicit solvent, possibly indicating that other factors, such as, for example, accurate hydrogen bonding, could be more important.

Finally, to quantify the possible differences from the various water models on the structure of water itself, and also to relate to experimental results, we calculated the oxygen−oxygen radial distribution function (RDF) from pure water simulations. As shown in Figure 4, the radial distribution functions of the two TIP3P models are very close, and both are significantly worse than TIP4P when compared to the experimental curve from Soper.[28] The average densities over the 100 ns simulations are 1001.7 ± 1.3 kg/ m^3 and 1014.7 ± 1.4 kg/ m^3 for original TIP3P and CHARMM-modified TIP3P, respectively.

Discussion

There are no significant differences in protein backbone dihedral angles when using the CHARMM-specific TIP3P model compared to the original TIP3P with only a single Lennard-Jones interaction site, and at least for the dihedrals, the results are very close to TIP4P. In terms of long-time structural stability, using the CMAP correction term really does seem to do what it was intended to do, even on timescales where problems frequently start to show; increasing simulation time to the 100 ns scale still produces improvements consistent with those originally observed on a single nanosecond scale.[7]

Both from accuracy and computational points of view, water models can be important. CHARMM typically uses a slightly modified version of TIP3P that includes Lennard-Jones interactions on all atoms, while the original Jorgensen model[18] only does it on the water oxygen. The classical argument in the latter case is that the hydrogens are extremely small, and that the Lennard-Jones potential anyway is an approximation. Since water can account for 90% of the interactions in a typical biomolecular simulation, GROMACS includes special nonbonded kernels that can take the absence of Lennard-Jones interactions on hydrogens into account to accelerate those interactions. When first implementing the CHARMM force field in GROMACS, we considered writing similar kernels for the alternative water model.

In general, minor changes in water models can be quite important. For many features such as hydration entropies, enthalpies, or heat capacities, the choice of water model is even much more important than the rest of the force field.[29] As evident from Figure 4, both the original and CHARMM TIP3P models deviate significantly from TIP4P or the experimental results, but the differences between the two models are minimal. Both models also appear equally good at stabilizing the protein structure, so rather than implementing a separate set of kernels—which would still be slightly slower than the original ones—we would rather advocate the use of the standard Jorgensen TIP3P model, without Lennard-Jones interactions on the hydrogens (but both choices are available). This does not rule out the possibility of model differences being significant in some cases, but for critical applications, we would anyway rather recommend TIP4P, which is only 7% slower than TIP3P in GROMACS.

As with the different water models, the choice of explicit versus implicit solvent depends on the questions being addressed. If accurate dynamics or, for example, exact hydrogen bond patterns are important, explicit solvent is the natural choice. However, longer timescales can be reached with an implicit solvent, and since solvent relaxation is instantaneous, it can also provide better sampling. This can be important for structural refinement where sampling is critical—provided the lowest free energy state of the force field is close to the native state.

It is reassuring that there does not appear to be any significant difference from the use of virtual sites to extend the time step; no negative trends are visible when measuring

the degree of structural divergence going from 2 to 4 fs. Even with implicit solvent and a 5 fs time step, accuracy is maintained, and the effect of the CMAP correction term is virtually the same as for the explicit solvent (Table 2). Regardless of the choice of solvent or water model, these results seem to indicate that the CHARMM force field works remarkably well with the combination of long timesteps enabled by virtual sites and implicit solvent.

It is interesting to see how the performance depends on both the solvent model and virtual interaction sites. Protein G itself consists of some 900 atoms, and with 8734 waters added, the total number of atoms exceeds 27 000 and 35 000 for TIP3P and TIP4P, respectively. Runs were performed on a 2.66 GHz quad-core Intel Nehalem, using long 1.2 nm cutoffs, PME calculated every step, and Parinello−Rahman pressure scaling, as described in the Methods section. The use of CHARMM-specific TIP3P resulted in a performance of 3.3 ns/day, while standard TIP3P reaches 5.9 ns/day and TIP4P 5.5 ns/day. Combining TIP3P with virtual sites and 4 fs steps yielded 11.3 ns/day with maintained accuracy. Finally, the (relatively expensive) OBC implicit solvent model with virtual sites and 5 fs time steps reaches a full 250 ns/day, with only marginal effects on quality.

To truly assess refinement, a more stringent test would be to take a diverse set of protein structure models, such as those produced at the biannual CASP experiment, and see whether it is possible to systematically move these closer to the native state. What we have presented here might arguably represent an easier problem, since our starting structures were produced from the native state using high-temperature simulations. The question is whether or not this means that there in some sense is an "easier" way back to the native state; that is, are "real" homology models more difficult to refine? This is a highly important question, but answering it is beyond the scope of this force field study. However, the example studied here provides promising signs that (1) refinement could indeed be possible with reasonable amounts of simulation time, (2) different solvent models might be important at different degrees of divergence from the sought native state, and (3) correction maps appear to be a universal improvement.

Conclusions

As first observed by MacKerrel et al., the improvement from the correction maps term is significant considering the efforts that have gone into parametrizing current force fields. We find it quite striking that it seems to hold across the line in our tests, regardless of water model or even implicit solvent. The success of combining an implicit solvent model and long time steps using CHARMM27 with correction maps (a computationally very appealing combination) suggests that it is a promising setup, for example, for protein refinement simulations where the sampling efficiency is one of the limiting factors. The fact that the correction maps seem to be a close-to-universal improvement also suggests that it would be interesting to evaluate the effect of similar correction terms for other parameter sets, which is a direction we intend to pursue in the future. The implementation presented here is already available in the public GROMACS git repository (see www.gromacs.org for information) and will be officially supported as of GROMACS 4.1.

Acknowledgment. This work was supported by grants to E.L. from the European Research Council (209825), the Swedish Foundation for Strategic Research, and the Swedish Research Council. Supercomputing resources were provided by National Science Foundation award CNS-0619926 to Stanford University.

References

(1) Wang, J.; Cieplak, P.; Kollman, P. *J. Comput. Chem.* **2000**, *21*, 1049–1074.

(2) Duan, Y.; Wu, C.; Chowdhury, S.; Lee, M.; Xiong, G.; Zhang, W.; Yang, R.; Cieplak, P.; Luo, R.; Lee, T.; Caldwell, J.; Wang, J.; Kollman, P. *J. Comput. Chem.* **2003**, *24*, 1999–2012.

(3) Oostenbrink, C.; Villa, A.; Mark, A. E.; Van Gunsteren, W. F. *J. Comput. Chem.* **2004**, *25*, 1656–1676.

(4) MacKerell, A. D.; et al. *J. Phys. Chem. B* **1998**, *102*, 3586–3616.

(5) Jorgensen, W. L.; Maxwell, D. S.; Tirado-Rives, J. *J. Am. Chem. Soc.* **1996**, *118*, 11225–11236.

(6) Kaminski, G. A.; Friesner, R. A.; Tirado-Rives, J.; Jorgensen, W. L. *J. Phys. Chem. B* **2001**, *105*, 6474–6487.

(7) MacKerell, A. D., J.; Feig, M.; Brooks, C. L. *J. Comput. Chem.* **2004**, *25*, 1400–15, 3d.

(8) van der Spoel, D.; Lindahl, E. *J. Phys. Chem. B* **2003**, *117*, 11178–11187.

(9) Feenstra, A.; Hess, B.; Berendsen, H. *J. Comput. Chem.* **1999**, *20*, 786–798.

(10) Zhu, J.; Fan, H.; Periole, X.; Honig, B.; Mark, A. *Proteins* **2008**, *72*, 1171–1188.

(11) Chopra, G.; Summa, C.; Levitt, M. *Proc. Natl. Acad. Sci. U. S. A.* **2008**, *105*, 20239–20244.

(12) Misura, K.; Baker, D. *Proteins* **2005**, *59*, 15–29.

(13) Chen, J.; Im, W.; Brooks, C. L. *J. Comput. Chem.* **2005**, *26*, 1565–1578, 3rd.

(14) Brooks, B. R.; Bruccoleri, R. E.; B. D. Olafson, D. J. S.; Swaminathan, S.; Karplus, M. *J. Comput. Chem.* **1983**, *4*, 187–217.

(15) Derrick, J. P.; Wigley, D. B. *J. Mol. Biol.* **1994**, *243*, 906–18.

(16) DeLano, W. L. *The PyMOL Molecular Graphics System*, v1.1r1; DeLano Scientific: Palo Alto, CA, 2002.

(17) Berman, H. M.; Westbrook, J.; Feng, Z.; Gilliland, G.; Bhat, T. N.; Weissig, H.; Shindyalov, I. N.; Bourne, P. E. *Nucleic Acids Res.* **2000**, *28*, 235–42.

(18) Jorgensen, W. L.; Chandrasekhar, J.; Madura, J. D.; Impey, R. W.; Klein, M. L. *J. Chem. Phys.* **1983**, *79*, 926–935.

(19) Onufriev, A.; Bashford, D.; Case, D. *Proteins* **2004**, *55*, 383–394.

(20) Essmann, U.; Perera, L.; Berkowitz, M. L.; Darden, T.; Lee, H.; Pedersen, L. G. *J. Chem. Phys.* **1995**, *103*, 8577–8593.

(21) Bussi, G.; Donadio, D.; Parrinello, M. *J. Chem. Phys.* **2007**, *126*, 014101.

(22) Parrinello, M.; Rahman, A. *J. Appl. Phys.* **1981**, *52*, 7182–7190.

(23) Snow, C.; Nguyen, H.; Pande, V.; Gruebele, M. *Nature* **2002**, *420*, 102–106.

(24) Hess, B. *J. Chem. Theory Comput.* **2007**, *4*, 116–122.

(25) Phillips, J.; Braun, R.; Wang, W.; Gumbart, J.; Tajkhorshid, E.; Villa, E.; Chipot, C.; Skeel, R.; Kale, L.; Schulten, K. *J. Comput. Chem.* **2005**, *26*, 1781–1802.

(26) Steinbach, P.; Brooks, B. *J. Comput. Chem.* **1999**, *15*, 667–683.

(27) Hess, B. *J. Chem. Phys.* **2002**, *116*, 209–217.

(28) Soper, A. *Chem. Phys.* **2000**, *258*, 121–137.

(29) Hess, B.; van der Vegt, N. *J. Phys. Chem. B* **2006**, *110*, 17616–17626.

CT900549R